# Xplo-SA9T: Optimization of Sorbent Technology With Existing and New Amine Variants for Carbon Dioxide Removal and Humidity Control

John R. Tidwell[1]
*XploSafe, Stillwater, OK 74074*

Nicholas F. Materer [2]
*Department of Chemistry, Oklahoma State University, Stillwater, OK 74078*

Evgueni B. Kadossov[3], Hanna R. Anderson[4], Zachary A. Brown[5], Michael L. Teicheira[6], Shoaib Shaikh[7]
*XploSafe, Stillwater, OK 74074*

*and*

Allen W. Apblett[8†]
*Department of Chemistry, Oklahoma State University, Stillwater, OK 74078*

**Scrubbing of the spacesuit air stream to control humidity and regulate carbon dioxide ($CO_2$) relies on amine-loaded resins, colloquially known as sorbents. The efficacy of Rapid Cycle Amine technology relies on the propensity of nitrogens toward adsorption of $CO_2$ while simultaneously offering regenerative properties under vacuum or positive pressure. The commonly utilized sorbent, SA9T, was recreated and evaluated further to increase stability and serve as a benchmark comparison for newly synthesized amine sorbent technologies. Ongoing storage studies with eight different environments will allow the development of applicable storage protocols and provide insight into possible ammonia generation pathways. Attempts to alleviate the known issues with SA9T included the alteration of the primary amine (tetraethylenepentamine), the choice of resin, and the particle size distribution. In-house $CO_2$ breakthrough experiments were conducted using a specialized apparatus that can simulate spacesuit conditions, offering high-quality triplicate capacity analysis affording direct comparison to known adsorbents in the literature. Thermo-Desorption Gas Chromatography Mass Spectrometry studies on the synthesized materials revealed any reagent or solvent off-gassing while Nuclear Magnetic Resonance spectroscopy tracked the stability of the bound amine. Scanning Electron Microscope images of sieved materials provided a more accurate size interpretation facilitating synthetic design and pressure drop elimination. All efficient sorbents were synthesized to a commercial batch scale subsequent to evaluation including Xplo-SA9T.**

[1] Research Scientist I, XploSafe, and 712 Eastgate St., Stillwater, OK 74074.
[2] Professor of Chemistry, Department of Chemistry, 318 Physical Sciences I, Stillwater, OK 74078
[3] Research Scientist III, XploSafe, Stillwater, OK 74074.
[4] Research Associate, XploSafe, Stillwater, OK 74074.
[5] Analytical Laboratory Manager, XploSafe, Stillwater, OK 74074.
[6] Operations Manager, XploSafe, Stillwater, OK 74074.
[7] Product Development Specialist and Program Manager, XploSafe, Stillwater, OK 74074.
[8] Professor of Chemistry, Department of Chemistry, 318 Physical Sciences I, Stillwater, OK 74078.
[†] Deceased, 29 May 2023

## Nomenclature

| | | |
|---|---|---|
| *ASTM* | = | American Society for Testing and Materials |
| *$CO_2$* | = | carbon dioxide |
| *EVA* | = | extravehicular activity |
| *$H_2O$* | = | water |
| *ISS* | = | International Space Station |
| *MEMS* | = | microelectromechanical systems |
| *MMPA* | = | methyl methacrylate tetraethylenepentamine |
| *mmHg* | = | millimeters of mercury, unit of pressure |
| *NASA* | = | National Aeronautics and Space Administration |
| *$N_2$* | = | nitrogen gas |
| *NDIR* | = | non-dispersive infrared |
| *NMR* | = | Nuclear Magnetic Resonance |
| *$O_2$* | = | oxygen gas |
| *ppm* | = | parts per million, unit of concentration |
| *RCA* | = | Rapid Cycle Amine |
| *RCRS* | = | Regenerable Carbon Dioxide Removal Systems |
| *RH* | = | relative humidity |
| *SA9T* | = | Solid Amine Adsorbent (Proprietary Adsorbent) |
| *SBIR* | = | Small Business Innovation Research |
| *SEM* | = | Scanning Electron Microscope |
| *TEPA* | = | tetraethylenepentamine |
| *SS* | = | stainless steel |
| *TD* | = | Thermal Desorption |
| *TD-GCMS* | = | Thermal Desorption Gas Chromatography-Mass Spectrometry |
| *UHP* | = | ultra-high purity |

## I. Introduction

Sorbent technologies rely upon the adsorption or absorption of gaseous or liquid species on or within a material. Adsorbents are relied upon within enclosed spaces that lack adequate ventilation and are saturated with byproducts of human metabolism, such as respiration and $CO_2$ production. These enclosures of interest range from common automobile cabins to more elaborate vessels such as submarines and space flight systems. The atmosphere on Earth is comprised of ~300 ppm $CO_2$, and when concentrations surpass 1000 ppm humans can feel ill.[1] Further prolonged exposures to high concentrations can result in dizziness (1%), lethargy (2%), deterioration of the central nervous system 30,000 ppm, and ultimately respiratory failure 50,000 ppm.[1] The concern for countering the effects of $CO_2$ production stems from the measured human metabolic output of 0.3－7.8 g/min during spaceflight missions or EVAs.[2] The most common method of removal of $CO_2$ is by its reaction with solid alkaline salts, such as calcium or lithium hydroxide, to form carbonate and bicarbonate salts.[3,4] With terrestrial and space applications, the commonly used $CO_2$ removal method consists of regenerable molecular sieve (within the ISS) and silver oxide (within the EMU) systems.[5,6] $CO_2$ can be removed from gas streams due to the lack of polarity in species such as $N_2$ and $O_2$.[7] Incorporation of nitrogen into sorbent technology is common for $CO_2$ capture as the dipole－quadrupole interaction facilitates capture and sequestration.[8-10] Most adsorbents used are expendable by definition as their regeneration is not kinetically favorable or their reaction is not sufficiently fast for enclosed environments such as spaceflight. Examples of patents involving $CO_2$ scrubbing of flue gas from coal-fired power plants date to the 1930's whereas amine-based $CO_2$ scrubbing was first evaluated in 1991.[11,12] Primary amines have the highest affinity for acidic $CO_2$ due to their basic and nucleophilic behavior.[13] Secondary amines have less $CO_2$ affinity based on lower alkalinity; however, they offer more regeneration based on the weaker introduced chemical interaction. Tertiary amines are the least basic and therefore least attracted to $CO_2$. At high temperatures, urea formation occurs with primary amines but can be suppressed with the presence of adequate humidity.[14] In general, due to cost and functionality a mixed amine adsorbent with predominately secondary amines offers flexibility and tunability for $CO_2$ capture.[15-17] Final considerations with amine adsorbent technologies rely on material regeneration with increased scrutiny due to bed-size restrictions and exposure limitations.[18-21]

## II. Background

SA9T, first manufactured by Hamilton-Sundstrand, has been used in American Aerospace $CO_2$ removal since its introduction at the turn of the 21st century, as a more efficient replacement for the existing amine technology used in the RCRS.[22-24] The material, manufactured by the surface-coating of TEPAN onto polymeric resin beads, has been well-documented in previous literature.[25-29] During the preliminary testing for SA9T variants, over 25 variations of carbon-based support materials were explored all with less than 70% of the maximum $CO_2$ adsorption capacity of SA9T.[28] Within the last decade, SA9T has been evaluated by amine swingbed payload testing on the ISS, modified heated $CO_2$ removal systems, and multiple NASA RCA system revisions since 2006.[21,30-32] The RCA-based systems rely on the ability of SA9T to adsorb $CO_2$ and humidity within a two-sorbent bed system.[33] This concept that requires one bed to remain active for adsorption, while the alternate bed undergoes regeneration by vacuum. The unifying concept for the beds includes a bed switching mechanism (pneumatically actuated linear motion spool valves) and reticulated aluminum foam that adds support and a means of heat transfer for the SA9T beads. The system bed sizes differ between manufacturers, varying from ~700－1000 $cm^3$ per bed.[21,32-34] The major pitfalls of SA9T include the propensity for ammonia off-gassing and the toxic nature of acrylonitrile used during the amine modification.[26,34] Consequently, variants have been extensively explored for $CO_2$ capture including liquid amine sorbents, carbon-based monoliths, and various synthetically modified amines.[35-39] In this work, we report a reproduced version of SA9T with further characterization and continued work toward a new amine adsorbent variant.

## III. Equipment Design

A specialized dosing rig was used to accommodate the $CO_2$ breakthrough capacity testing. The rig (**a, Figure 1**) consists of 5 Dakota Instruments digital mass flow controllers, ¼" SS tubing with Swagelok SS fittings, dual fritted glass washing bottles charged with $H_2O$, and the corresponding sensors and electrical components. The rig was designed to afford both accurate and precise triplicate measurements of various sorbents and employs glass TD tubes as a sorbent carrier (**b, Figure 1**). The sorbent column length can be manipulated within the tube to allow for a comparable mass if required. The flow diagram in **Figure 2** illustrates the placement of major components within the rig.

a) 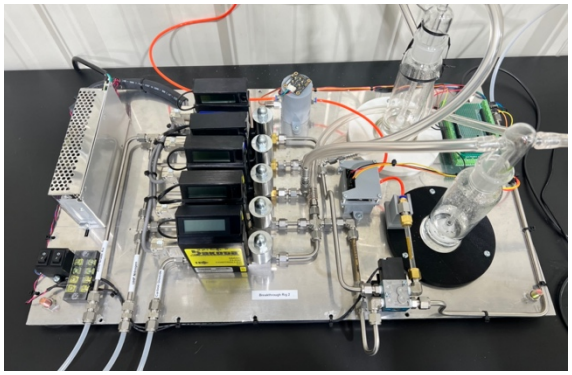 b) 

**Figure 1: $CO_2$ breakthrough rig (a) and packed sorbent (Xplo-SA9T) within standard glass TD tube (b).**

A secondary $CO_2$ breakthrough rig was fabricated to compare the reproducibility of the sorbent measurements. The second breakthrough rig used identically rated flow controllers, power supply, cross valve, sensors, and fritted glass washing bottles. Both rigs were loaded with the identical software and connected to two different computers for serial input. Sorbent samples of the same batch of Xplo-SA9T were loaded onto each rig and ran by one technician at 10,500 ppm $CO_2$ and 52% RH. The breakthrough capacity results indicated 1.970 and 1.978 mmol/g for both rigs. Each tube was regenerated by ~10 psi $N_2$ at 60 ˚C for 2 hours and placed back on the rigs a different day. The Xplo-SA9T samples were rerun until breakthrough by a different technician and the $CO_2$ breakthrough capacities were calculated as 1.773 and 1.769 mmol/g. These measurements by two different technicians, rigs, and days indicate a precision average of 0.004 mmol/g validating internally the reproducibility of the measurements.

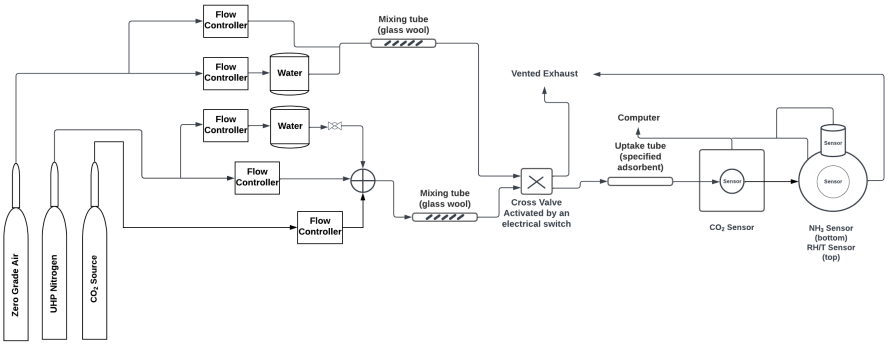


**Figure 2: Flow Diagram for the $CO_2$ Breakthrough Rig.**

## Experimental Details

Triplicate blank capacities were collected daily before any sorbent testing, ensuring the proper function of the equipment. The blanks consist of a single glass 3.5" x ¼" (89 x 6.35 mm) glass TD tube that is pre-conditioned in a tube conditioner. The equipment consists of a specialized breakthrough rig (**a, Figure 1**) built with 5 Dakota Instruments digital gas mass flow controllers, ¼" stainless steel tubing with Swagelok fittings, 2 fritted glass washing bottles, an electronically stimulated cross valve, a power supply, Arduino serial logger, and the desired sensors. The flow controllers direct UHP nitrogen, ultra zero-grade air, and calibrated carbon dioxide gas to achieve a stabilization rate of 100 mL/min zero-grade air, and a 100 mL/min calibrated $CO_2$/nitrogen/air concentration. Both the stabilization flow and the calibrated gas flow are equipped to adjust humidity through the fritted glass wash bottles. The sensors equipped within this study include dual-channel NDIR gold-plated optical $CO_2$ sensors with three varying ranges (0 −2,000, 0−5,000, and 0−50,000 ppm), a MEMS $NH_3$ sensor (0−100 ppm), and a combined silicon bandgap RH/temperature sensor (0−100% RH, −40−123.8 ˚C). The blanks will ensure the calibrated dosing rate for $CO_2$ is within reason of the specific calibrated gas data sheet (9.978 ± 2 % $CO_2$/air). The $CO_2$ sensors have an accuracy of 75 ppm or 10% of the reading, whichever is greater. Three $CO_2$ dosing rates were used throughout experimentation to introduce a wide range of potential metabolic rates: 500 (0.38 mmHg), 2800 (2.1 mmHg), and 10,500 (7.98 mmHg) ppm.

$$molar\ volume\left(\frac{L}{mol}\right) = \frac{temperature\ (K) \times 8.314\left(\frac{L \cdot kPa}{K \cdot mol}\right)}{101.325\ kPa}$$

$$CO_2\ per\ volume\ of\ gas\left(\frac{g}{L}\right) = \frac{CO_2\ concentration\ (ppm) \times \left(\frac{vol\ CO_2\ 1 \times 10^{-6}\ L}{total\ gas\ volume\ L}\right) \times CO_2\ molar\ mass\left(\frac{g}{mol}\right)}{molar\ volume\left(\frac{L}{mol}\right)}$$

$$total\ amount\ of\ CO_2(mg) = time\ (min) \times flow\ rate\left(\frac{L}{min}\right) \times CO_2\ per\ volume\ of\ gas\left(\frac{g}{L}\right) \times unit\ conversion\left(\frac{1000\ mg}{1\ g}\right)$$

$$CO_2\ per\ total\ area = \frac{area\ of\ CO_2\ adsorbed\ (area\ of\ full\ rectangle\ -\ area\ of\ integration)}{area\ of\ full\ rectangle}$$

$$mmol\ CO_2 = total\ amount\ of\ CO_2\ adsorbed\ (mg) \times \frac{1\ g}{1000\ mg} \times \frac{1\ mol}{44\ g} \times \frac{1000\ mmol}{1\ mol}$$

$$capacity\ of\ sorbent\ at\ breakthrough\ (0\ to\ 99\%) = \frac{mmol\ of\ CO_2}{g\ of\ sorbent}$$

$$total\ amount\ of\ CO_2\ adsorbed\ (mg) = total\ amount\ of\ CO_2\ (mg) \times \left(\frac{CO_2}{total\ area}\right)$$

**Equation Set 1: Example calculation for capacity of sorbent at 0−99% breakthrough.**

Breakthrough sample analysis was collected at the 99% breakthrough interval. For the sample size, approximately 70 －100 mg of sorbent dependent on type and particle size, a flow rate of 100 mL/min $CO_2$/nitrogen was chosen, and a stabilization gas of zero-grade air was used. Each sample consists of a pre-measured 14 mm x 4 mm sorbent bed within a TD tube. The average time to reach 99% breakthrough for one sample occurs typically within an hour dependent on the concentration of $CO_2$ in the gas stream. In comparison to the literature, each sample set was exposed to a humid stream specified at 52% RH and 2,800 ppm $CO_2$ for 60 minutes. A list of equations used to calculate $CO_2$ breakthrough capacity is shown in **Equation Set 1** where temperature, $CO_2$ concentration in ppm, flow rate, time, and mass are collected during a sample set. During data manipulation, once the concentration is normalized relative to the percent breakthrough it is plotted against time. This plot allows for the calculation of "$CO_2$ per total area". The breakthrough curve is illustrated in **Figure 3** as an example of this process. During analysis, all sorbent samples should display a visible plateau where all incoming $CO_2$ gas passes through the sorbent and stabilizes across the sensor. The mass is comparable when packing to the 4 mm x 14 mm sorbent bed size; however, it is measured to the 10-thousandth during tube packing.

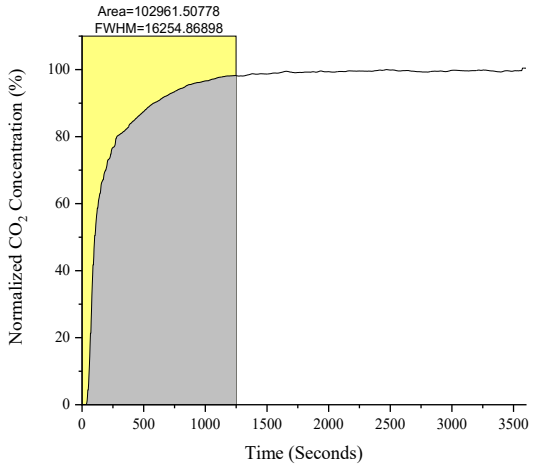


**Figure 3: Graphical example of data for $CO_2$ breakthrough capacity calculation (highlighted area is 0－99% breakthrough).**

Sorbent regeneration proceeds *via* regeneration within the TD tube, either by positive flow or under a controlled vacuum. Positive pressure regeneration occurs at room temperature on the designed breakthrough rig with zero-grade air or with UHP nitrogen at 60 ˚C in a Markes TC-20 tube conditioner for 2 hours. Vacuum regeneration is achieved using a standard direct-drive rotary-vane vacuum pump fitted with provisions for a TD-tube attachment, vacuum gauge, and two single-stage subatmospheric regulators to hold a near-constant 1.00 torr vacuum. Data collection occurs by first running the sorbent until the $CO_2$ breakthrough followed by performing the desired regeneration technique. The subsequently measured 99% breakthrough capacity is a true post-saturation and regeneration breakthrough capacity.

Amine manipulations were performed under an inert atmosphere where required. Solvents were purchased from commercial vendors and used as such. Reagents were purchased from commercial vendors and further purified when required. Chloroform-$d^3$ for NMR spectroscopy was used as purchased from Fisher Scientific and used as received. The SEM used is a ThermoFisher Scientific FEI Quanta 600 FEG Mk2 ESEM (2006). The nominal resolution is 10 nm for a tin ball standard. Any multinuclear NMR spectra were recorded on a Bruker AVANCE 400 MHz instrument. TD-GC/MS analysis was completed using an Agilent Technologies 6890N Gas Chromatograph, a Hewlett Packard 5973 Mass Selective Detector, and a Markes TD-100 Thermal Desorber. Elemental analysis samples were sent to Atlantic Microlab and were evaluated with a Carlo Erba 1108 Analyzer. The purity of new complexes was established by $^1$H NMR spectroscopy and elemental analysis.

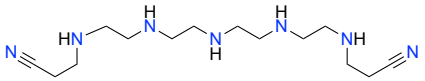

**Figure 4:** Structure of Xplo-SA9T.

**TEPAN**: Synthesized by a modified literature procedure.[25] $^1$H NMR (400 MHz, $CDCl_3$): δ (ppm) 2.93 (t, *J*= 6.0 Hz, 4H), 2.81－2.46 (m, 20H), 1.96 (bs, 5H)

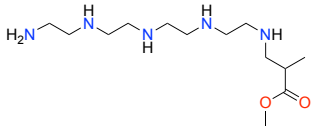

**Figure 5:** Structure of MMPA.

**MMPA**: Synthesis is proprietary. $^1$H NMR (400 MHz, $CDCl_3$): δ (ppm) 3.53 (s, 3H), 2.63－2.33 (m, 19H), 1.21 (s, 6H), 1.01 (s, 3H); Analysis Calculated (found) (%): C 53.95 (53.36), H 10.80 (10.79), N 24.20 (23.40)

## IV. Results and Discussion

### A. Synthesis of Xplo-SA9T

The synthesis of TEPAN from TEPA and two equivalents of acrylonitrile was carried out by a modified literature procedure (**Scheme 1**).[25] The corresponding amine (**Figure 4**) was further purified and loaded onto the corresponding polymer resin (Mitsubishi Diaion HP2MGL, 1.3 mL/g pore volume, 240 Å pore radius). The amine within Xplo-SA9T was further characterized by NMR spectroscopy to reveal complete chemical conversion, as well as to elucidate the species present in the liquid state (**Figure 6**). The NMR spectrum displays a triplet resonance at 2.93 that can be

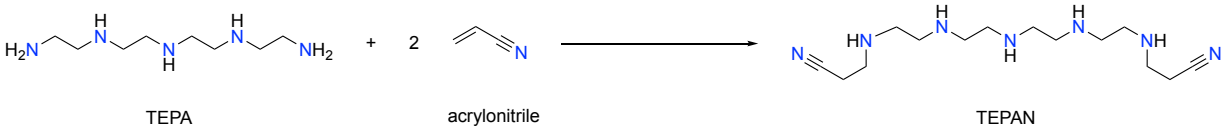


**Scheme 1: General reaction for the synthesis of TEPAN.**

attributed to the hydrogens of the β-carbon from the reacted acrylonitrile, the multiplet from 2.81－2.46 integrates with respective to all remaining non-amine hydrogens with the TEPAN molecule. The broad singlet resonance at 1.96 is indicative of amines and pertains to the five nitrogen-bound hydrogen atoms within TEPAN.[40] Triplicate TD-GC/MS analysis of the produced sorbent displayed spectroscopic peaks associated with the synthetic process; however, the solvents used during the amine synthesis were no longer present. Further purification of the sorbent reduced the major solvent impurities from resin loading; however, residual acrylonitrile could still be detected. Xplo-SA9T was scaled up to 2-kilogram batches, yielding 82% dried sorbent.

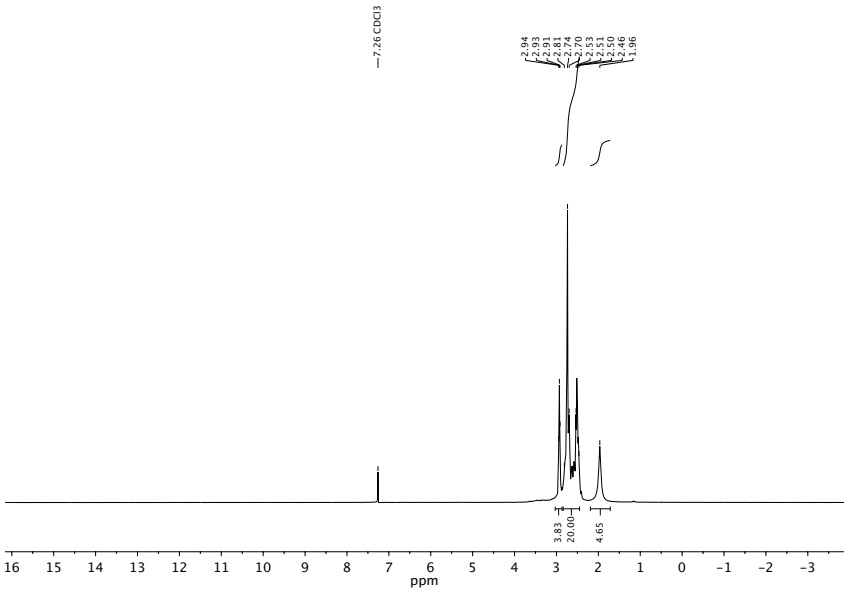


**Figure 6: $^{1}$H NMR spectrum of Xplo-SA9T.**

**Characterization by 0−99% total $CO_2$ breakthrough capacity of Xplo-SA9T**

The sorbent was tested for functionality by measuring 0−99% total $CO_2$ breakthrough capacity in a specialized dosing rig (**Figure 1,** and **Figure 2**). Initially, the sorbent was tested using a similar literature procedure as Monje and co-authors, utilizing 2800 ppm $CO_2$, 52% RH, and a 60-minute exposure time, with a reduced flow rate of 100 mL/min to accommodate the smaller adsorbent bed size of 4 mm x 14 mm.[27,41] The literature values for the 60-minute exposure result in a calculated $CO_2$ capacity of 0.422 ± 0.001 mmol/g for SA9T, whereas Xplo-SA9T revealed a $CO_2$ capacity of 1.037 ± 0.005 mmol/g. Further tests compared variations in inlet $CO_2$ ranging from 500−10,500 ppm $CO_2$ with breakthrough capacities of 0.53 ± 0.02 mmol/g and 1.97 ± 0.04 mmol/g (500 and 10,500 ppm, respectively). This result is further supported by the previous work of Hamilton Sundstrand where an increase in capacity was observed as inlet $CO_2$ concentration increased.

**Characterization for water uptake capacity of Xplo-SA9T**

Water uptake capacities for Xplo-SA9T were consistent [when compared to SA9T, (69 ± 1.0 g•kg−1)] for a humid stream coupled with $CO_2$. They were measured after dosing dry ~0.45g TD tube samples (evacuated below 1 torr) with 52% RH for 1 hour at a 100 mL/min flow rate. The triplicate samples were measured at 69 ± 1 $g \cdot kg^{-1}$ (water/sorbent) for a humid stream and 69 ± 2 $g \cdot kg^{-1}$ for a humid stream plus 10,500 ppm $CO_2$ simultaneous flow.

**Experimental design tests and validation**

A follow-up test to determine if sorbent bed volume (column length) affected the results was conducted with a triplicate analysis of three varying column lengths. 14, 20, and 26 mm (~85, ~138, and ~177 mg) columns were used with a 2,800 ppm $CO_2$ and 52% RH stream; experimental capacities were measured at 1.12 ± 0.02, 0.98 ± 0.06, and 0.99 ± 0.04 mmol/g, respectively. This minor difference in $CO_2$ uptake between bed sizes is attributed to the use of non-sieved material and supports a non-statistical change between bed sizes on the designed breakthrough rig.

**Characterization by 0−99% total $CO_2$ breakthrough capacity of Xplo-SA9T in different humidity levels**

To compare the effect of humidified vs. dry $CO_2$, an experiment was conducted where a dry bed was exposed to a dry stream of $CO_2$ until breakthrough by removing the humidification setup on the dosing rig while maintaining the same experimental flow rate of 100 mL/min. The experiment was conducted at 10,500 ppm $CO_2$ and displayed a non-statistical difference of 1.87 ± 0.02 mmol/g for the 0% humidity and 1.87 ± 0.04 mmol/g for the humid stream. Further tests at 52% RH and 2,800 ppm $CO_2$ were conducted to compare pre-humidified Xplo-SA9T vs dry Xplo-SA9T resulting in similar capacities (1.057 ± 0.009 and 1.037 ± 0.005 mmol/g, respectively).

**B. Synthesis of MMPA Sorbent a SA9T Variant**

Attempts to remove acrylonitrile from the synthetic process led to the inspiration for less toxic amine variants. A modified amine using 1 equivalent of methyl methacrylate was chosen for exploration and synthesized as MMPA (**Scheme 2**). The purified amine (**Figure 5**) was loaded in various ratios onto a polymer resin resulting in the formation

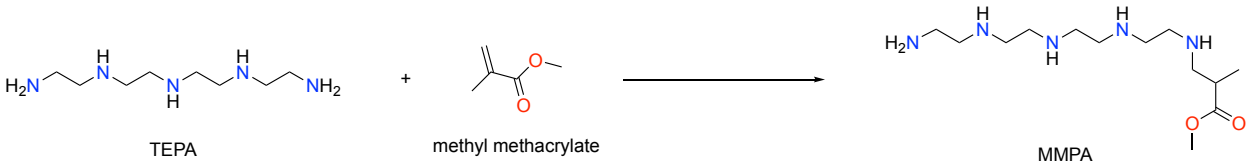


**Scheme 2: General reaction for the synthesis of MMPA.**

of a new material, MMPA sorbent. The amine was evaluated by NMR spectroscopy (**Figure 7**) and its identity was further supported by elemental analysis. NMR spectroscopy revealed a singlet resonance at 3.53 and 1.01 corresponding to the 6 hydrogens of the methyl groups within the bound methyl ester, a singlet at 1.21 pertaining to the amine bound hydrogen atoms, and a multiplet at 2.63—2.33 indicative of the remaining hydrogens found within the ethylene chain of the original TEPA amine and the methyl ester. Each ratio variant was tested for $CO_2$ adsorption and resulted in 0—99% $CO_2$ capacities of 1.46 ± 0.03 mmol/g to 2.21 ± 0.03 mmol/g at 52% RH, 10,500 ppm $CO_2$. MMPA-sorbent tested at 52% RH, 2800 ppm resulted in a capacity of 0.97 ± 0.07 mmol/g. The MMPA-sorbent was tested further by collecting 0—99% $CO_2$ breakthrough capacity in a non-humid stream on a dry adsorbent bed (freshly synthesized and evacuated below 1 torr) revealing a capacity of 1.06 ± 0.02 mmol/g at 2800 ppm $CO_2$. Water uptake capacities of MMPA-sorbent were measured after dosing dry ~0.34g TD tube samples (evacuated below 1 torr) with 52% RH for 1 hour at a 100 mL/min flow rate. The triplicate samples were measured at 88.0 ± 0.1 $g \bullet kg^{-1}$ (water/sorbent) for a humid stream and 60 ± 4 $g \bullet kg^{-1}$ for a humid stream with 10,500 ppm $CO_2$ simultaneous flow. TD-GC/MS analysis was conducted and revealed residual solvent remaining from synthesis and no major side-products.

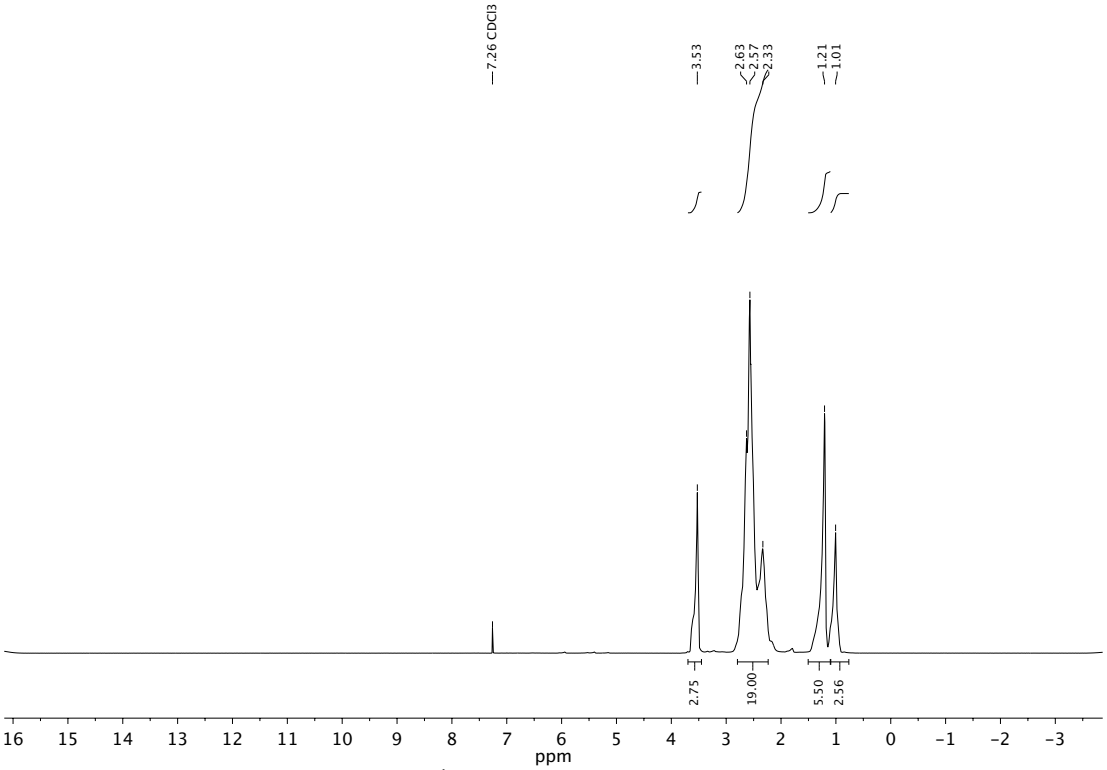


**Figure 7: $^1$H NMR spectrum of MMPA.**

**C. Characterization of Xplo-SA9T by SEM Imaging.**

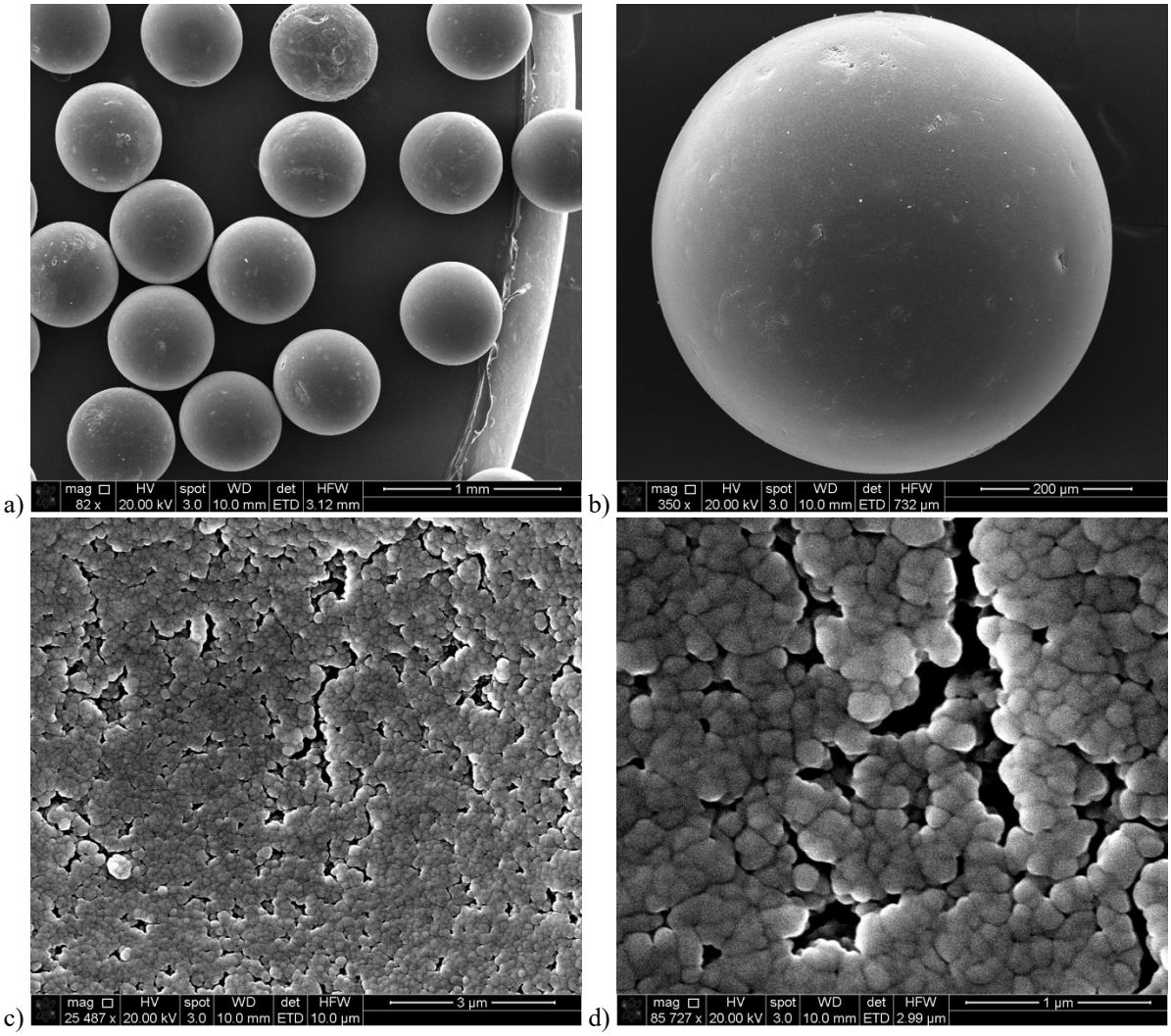


**Figure 8: SEM images of Xplo-SA9T sorbent beads: a) (82x) group of beads, b) (350x) single bead, c) (25,487x) bead surface, d) (85,727x) bead pores (magnification).**

The rigidity of the sorbent beads can be evaluated by a high-resolution microscope to aid in understanding the surface of the material. The material can be coated with gold nanoparticles and further evaluated by SEM. High-resolution (10 nm for a tin ball standard) SEM images were collected of the as-synthesized Xplo-SA9T sorbent (**Figure 8**) illustrating the appearance of the sorbent beads from 82－85,727x magnification. The sorbent pores are visible at both the 26,487x and 85,727x magnification. To reduce pressure variations within the xPLSS system the synthesized sorbent material is subjected to mechanical sieving with ASTM-E11-certified SS sieves. Adsorbent particles were mechanically sieved between 600－1000 µm [NO. 18 (1000 ± 40 µm) and NO. 30 (600 ± 25 µm)] particle size as seen in the SEM imaging (**a－e, Figure 9**). The non-sieved material ranges from a measured 427.0 µm to 709.5 µm whereas sieved material ranges from 577.4 µm to 625.2 µm measured by SEM imaging. To evaluate the overall sample lot sizing, a survey (**c. Figure 9**) was conducted on the SEM mount illustrating similar size distribution between the entire sorbent lot.

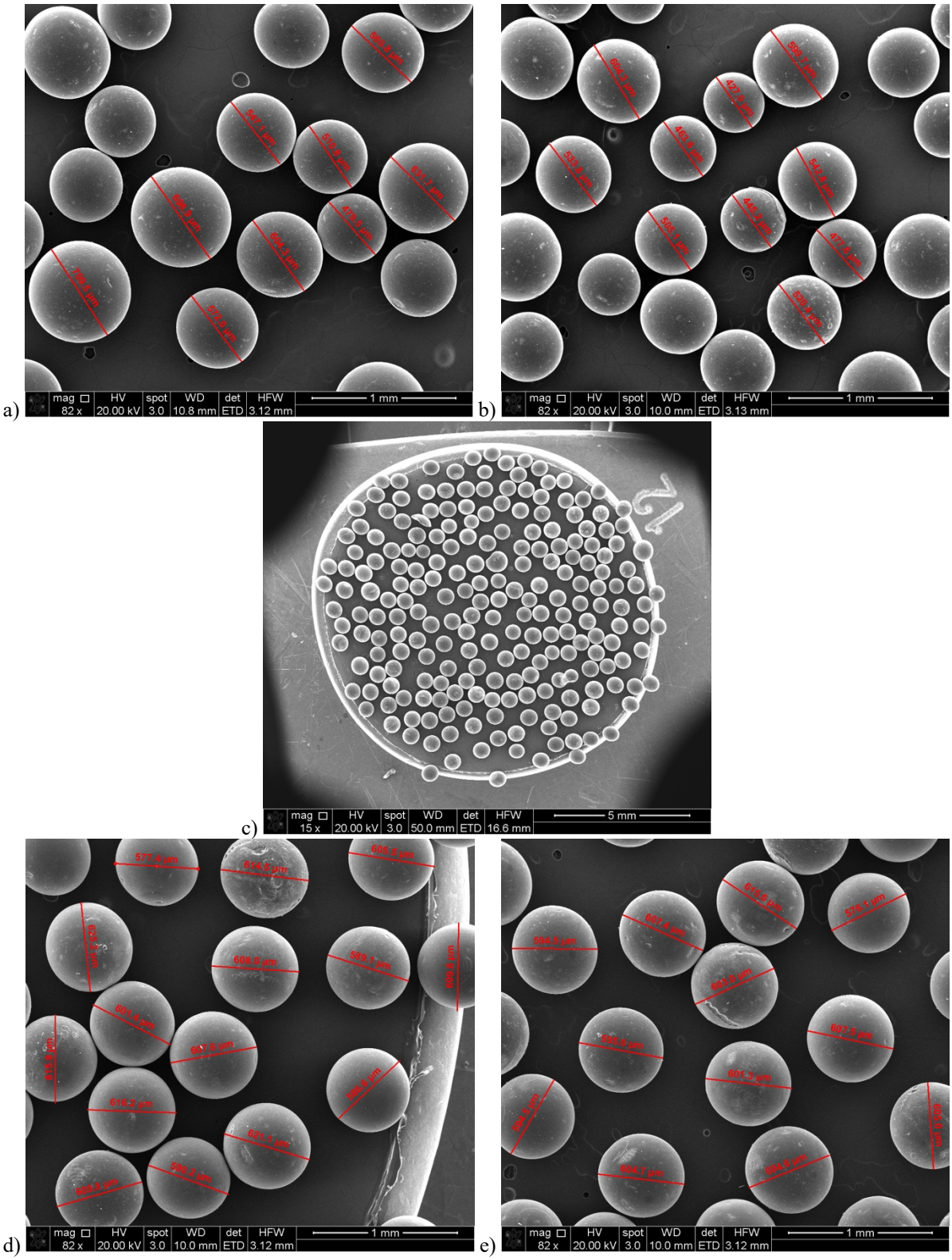


**Figure 9: SEM images of non-sieved and sieved Xplo-SA9T: a) and b) non-sieved, c) survey of sieved Xplo-SA9T, d-e) sieved Xplo-SA9T.**

## D. Sorbent Regeneration

Regeneration of material inside TD tubes is commonly performed with a tube conditioner by flowing UHP $N_2$ at 10 psi across the tubes. Temperature degradation of the amine loaded within the sorbent is possible; therefore, the tube conditioner was set to regenerate at 60 ˚C for 2 hours.[42] Xplo-SA9T was loaded into glass TD tubes and ran until breakthrough, at which point the tubes were regenerated with a tube conditioner. For the breakthrough capacity experiment, a $CO_2$ concentration of 500 ppm and 52% RH was used with a flow rate of 100 mL/min. The initial capacity for Xplo-SA9T was noted as 0.53 ± 0.02 mmol/g at 500 ppm $CO_2$, and once regenerated, the capacity fell by ~5% to 0.51 ± 0.02 mmol/g (example, **Figure 10)**. Multiple regeneration cycles from the same triplicate samples were performed with the tube conditioner, and after five regeneration cycles, the material remained useful with ~88% of its initial capacity remaining (0.47 ± 0.01 mmol/g).

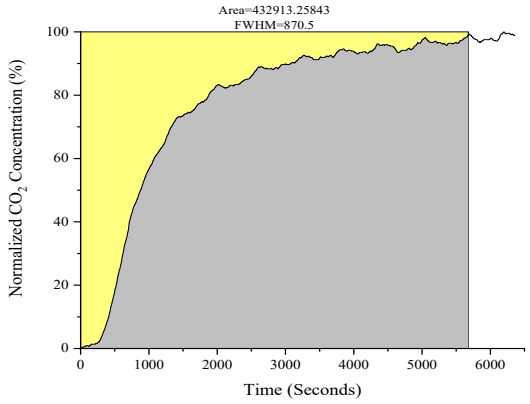


**Figure 10: $CO_2$ breakthrough capacity after regeneration of Xplo-SA9T with positive nitrogen flow at 60 ˚C for 2 hours.**

Regeneration on the breakthrough rig utilizing positive gas flow (100 mL/min zero-grade air) was proven possible at 25.1 ˚C within an average of 2.03 hours (example, **Figure 11**). First, the sorbent was exposed to $CO_2$ until full breakthrough, then only the 100 mL/min flow of zero-grade air passed over the sample until a minimum plateau was reached. Second, a subsequent 0—99% capacity was collected and compared to the initial triplicate capacity for the same lot of sorbent at the same 52% RH and 2,800 ppm $CO_2$ concentration. The initial capacity for the Xplo-SA9T sorbent was measured at 1.037 ± 0.005 mmol/g compared to rig-regenerated material at 0.94 ± 0.06 mmol/g at 2800 ppm. This reveals a ~91% regeneration at ambient temperature with a flow rate of 100 mL/min of zero-grade air.

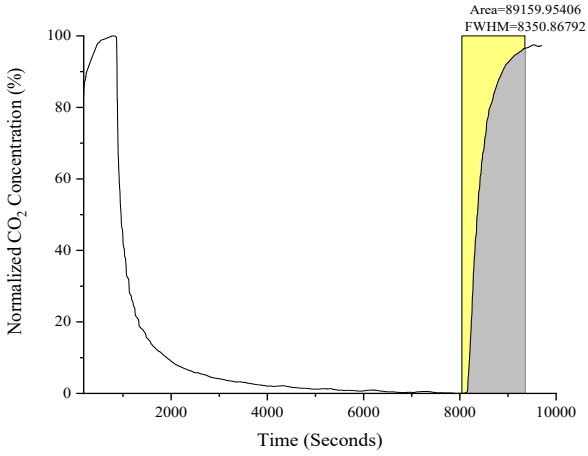


**Figure 11: Regeneration of Xplo-SA9T on the $CO_2$ breakthrough rig by positive pressure.**

Vacuum regeneration of adsorbent on the breakthrough rig first required the alteration of the rig itself. The stabilization-humid-air-flow was disabled to ensure any regeneration occurred only by vacuum. The samples were exposed to a concentration representative of a high metabolic rate (52% RH and 100 mL/min of 10,500 ppm $CO_2$) for each ~95 mg sorbent quantity.[2] Once a full breakthrough occurred (outlet concentration matches inlet concentration), the tubes were capped then transferred to the 1.00 torr vacuum rig and evacuated for a pre-determined time. After evacuation, they were returned to the breakthrough rig and immediately reexposed to identical test conditions. The initial adsorption capacities were calculated as were their corresponding regenerated capacities. These values are displayed in Figure 6; however, an example of initial capacity for Xplo-SA9T at 10,500 ppm $CO_2$ is 1.97 ± 0.04 when after evacuation at 1.00 torr for 2 minutes the corresponding capacity falls to 0.39 ± 0.01 mmol/g. An example of this run can be viewed in **Figure 12** illustrating the initial breakthrough and subsequent exposure and breakthrough following regeneration.

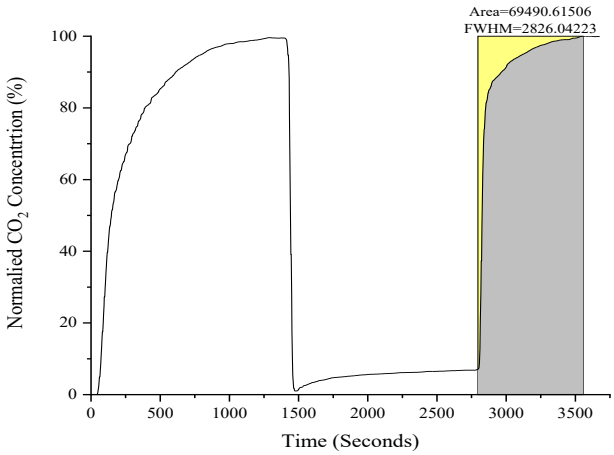


**Figure 12: Vacuum regeneration of Xplo-SA9T post-full breakthrough.**

Each time point was collected in triplicate for both Xplo-SA9T and MMPA sorbents. In addition, new material was used between time changes to ensure equivalent testing parameters across all samples. The results indicated by an 18-sample set of 600－1000 μm sieved Xplo-SA9T at 10,500 ppm $CO_2$ and 52% RH, divulged an initial 0－99% breakthrough capacity of 1.97 ± 0.06 mmol/g. When an 18-sample set of MMPA sorbent was evaluated using the same conditions an initial capacity of 2.18 ± 0.06 mmol/g was revealed. Each sorbent was exposed to a 1.00 torr vacuum for a chosen time interval of 2, 4, 6, 16, 26, or 60 minutes. The corresponding capacities after vacuum regeneration were plotted in **Figure 13** and logarithmic equations were fitted to the regeneration rate curves. The rates both support the theory that secondary amines regenerate better than primary amines while still possessing an affinity for $CO_2$.

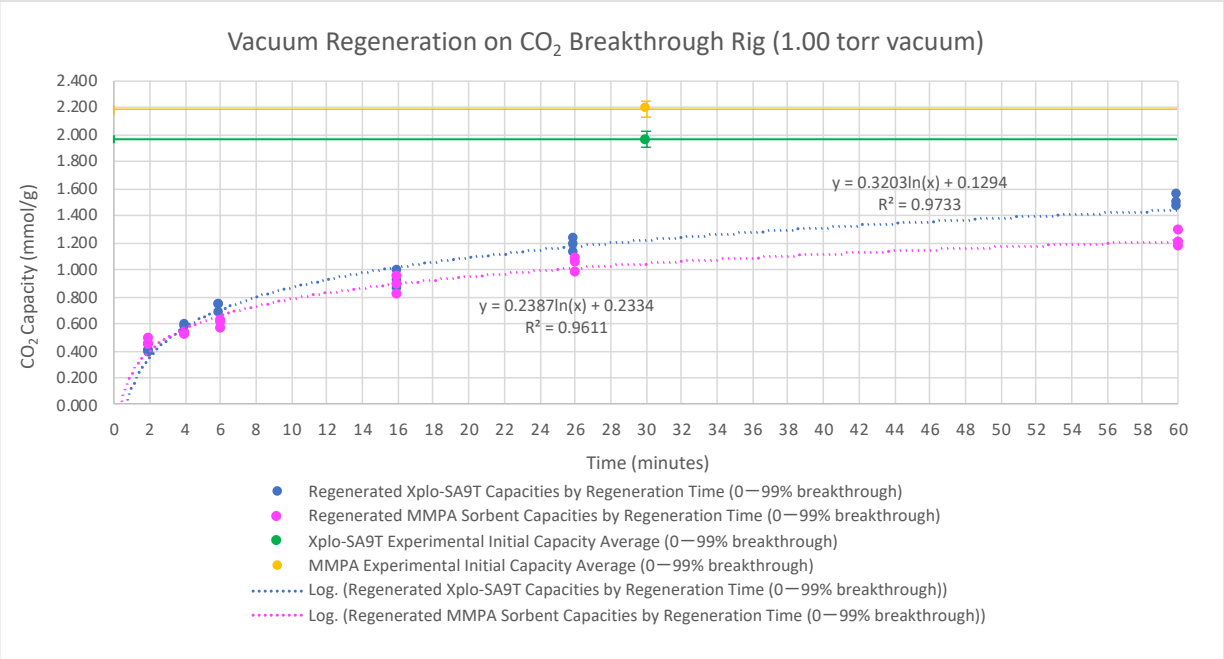


**Figure 13: Vacuum regeneration sorbent comparison of Xplo-SA9T and MMPA.**

The vacuum regeneration conditions for **Figure 13**, are all comprised of the same test conditions which include a timed evacuation regeneration study per adsorbent after total $CO_2$ breakthrough capacity. These tests were run at 10,500 ppm $CO_2$ and 52% RH.

All regeneration studies were conducted to screen the synthesized materials for their ability to regenerate in multiple environmental scenarios with application utility beyond the scope of only the current RCA systems. Varying metabolic $CO_2$ dosing rates were utilized as a consistent metabolic rate is unrealistic; however, anywhere materials were tested against each other or against literature values they were dosed at the same metabolic rate and humidity. Degradation timelines as well as performance metrics in the RCA system are not transferable to the characterization performed here and will be tested in the future on a regenerable swing-bed until material plateaus at a given rate or completely exhausts.

**Table 1:** Summary of $CO_2$ breakthrough capacities experimentally collected and literature SA9T values.[27]

| ***Material*** | ***Experimental Details*** | ***Capacity (mmol/g)**** |
|---|---|---|
| Literature SA9T | ~8g, 2800ppm $CO_2$, 52% humid stream, 20min exposure# | 0.311 ± 0.027 |
| Literature SA9T | ~8g, 2800ppm $CO_2$, 52% humid stream, 1h exposure# | 0.422 ± 0.001 |
| Xplo-SA9T sieved | ~95mg, 500 ppm $CO_2$, humid stream, breakthrough (1h) | 0.53 ± 0.02 |
| Xplo-SA9T sieved | ~95mg, 2800 ppm $CO_2$, humid stream, breakthrough (1h) | 1.037 ± 0.005 |
| Xplo-SA9T sieved | ~95mg, 2800 ppm $CO_2$, 0% humidity, breakthrough (1h) | 1.057 ± 0.009 |
| Xplo-SA9T sieved | ~95mg, 10,500 ppm $CO_2$, humid stream, breakthrough (1h) | 1.87 ± 0.04 |
| Xplo-SA9T sieved | ~95 mg, 10,500 ppm $CO_2$, 0% humidity, breakthrough | 1.87 ± 0.02 |
| MMPA-sorbent sieved | ~72 mg, 2800 ppm $CO_2$, humid stream, breakthrough (1h) | 0.96 ± 0.07 |
| MMPA-sorbent sieved | ~72 mg, 2800 ppm $CO_2$, 0% humidity, breakthrough (1h) | 1.06 ± 0.02 |
| MMPA-sorbent sieved | ~72 mg, 10,500 ppm $CO_2$, humid stream, breakthrough | 1.84 ± 0.01 |
| *MMPA-sorbent sieved (various wt% loadings)* | ~66-82 mg, 10,500 ppm $CO_2$, humid stream, breakthrough | 1.46 ± 0.03 -2.21 ± 0.03 |

** = mmol $CO_2$ per gram of sorbent, # = conducted at a flow rate of 2.9 L/min, humid stream is at 52% RH unless specified.*

## V. Conclusion

A new amine-based adsorbent was synthesized and explored in conjunction with the evaluation of Xplo-SA9T. Xplo-SA9T and the MMPA sorbent possess higher initial $CO_2$ capacities than expected and offer regeneration through vacuum or positive pressure flow. MMPA sorbent possesses a higher initial $CO_2$ adsorption capacity and similar regenerated capacity than the currently utilized and proven SA9T. A multitude of experiments were conducted for the adsorbents including triplicate initial $CO_2$ capacity, varying metabolic rate $CO_2$ capacities, column length $CO_2$ capacity effects, water uptake capacity, heated nitrogen regeneration, ambient compressed air regeneration, and vacuum regeneration. During breakthrough studies, ammonia was not shown during the data collection on the corresponding ammonia sensor (see Figure 2). Ammonia development is hypothesized to occur if the material is stored wet or stored for a long period of time. Xplo-SA9T was characterized by NMR spectroscopy, SEM imaging, and TD-GC/MS analysis. MMPA sorbent was characterized by NMR spectroscopy, TD-GC/MS analysis, and elemental analysis. Specialty dosing equipment was created and duplicated to ensure accurate and precise measurements for further variant studies. Future work includes long-term storage studies for Xplo-SA9T and MMPA-sorbent as well as further new amine variants and swing bed testing.

## Acknowledgments

Financial support for the project was provided by a NASA SBIR program under Contracts No. 80NSSC22PB246 and 80NSSC23CA167. The authors would like to acknowledge the contributions of Cinda Chullen, Bruce Conger, Lawrence Barrett, and all other NASA JSC employees who have provided wisdom, guidance, and funding for this work. In addition, the authors would like to recognize Dr. Allen W. Apblett, co-founder and President of XploSafe LLC until his tragic passing in May of 2023. Dr. Apblett laid the foundational groundwork for the research expanded upon here, and his contributions to XploSafe, Oklahoma State University (where he was employed as a professor since 1997), and chemistry, in general, will live on through his hundreds of publications, dozen patents, and countless undergraduate and graduate students who he mentored and instructed.

## References

1. Huang, Z.; Chen, Z.-b.; Ren, N.-q.; Hu, D.-x.; Zheng, D.-h.; Zhang, Z.-p., A novel application of the SAWD-Sabatier-SPE integrated system for CO2 removal and O2 regeneration in submarine cabins during prolonged voyages. *Journal of Zhejiang University-SCIENCE A* **2009,** *10* (11), 1642-1650.
2. Ewert, M.; Downs, M.; Keener, J. In *Developing a Daily Metabolic Rate Profile for Human Exploration Missions*, 50th International Conference on Environmental Systems: 2021.
3. Ahmadi, M.; Ghaemi, A.; Qasemnazhand, M., Lithium hydroxide as a high capacity adsorbent for CO2 capture: experimental, modeling and DFT simulation. *Scientific Reports* **2023,** *13* (1), 7150.
4. Costagliola, M. A.; Prati, M. V.; Perretta, G., Post combustion CO2 capture with calcium and lithium hydroxide. *Scientific Reports* **2022,** *12* (1), 10518.
5. Peters, B.; Westheimer, D. In *EMU METOX Performance Testing*, 48th International Conference on Environmental Systems: 2018.
6. Cmarik, G.; Knox, J.; Peters, W. In *4-Bed CO2 Scrubber–From Design to Build*, 2020 International Conference on Environmental Systems: 2020.
7. Koide, A.; Kihara, T., Intermolecular forces for D2, N2, O2, F2 and CO2. *Chemical Physics* **1974,** *5* (1), 34-48.
8. Li, P.-Z.; Zhao, Y., Nitrogen-Rich Porous Adsorbents for CO2 Capture and Storage. *Chemistry – An Asian Journal* **2013,** *8* (8), 1680-1691.
9. Olivares‐Marín, M.; Maroto‐Valer, M. M., Development of adsorbents for CO2 capture from waste materials: a review. *Greenhouse Gases: Science and Technology* **2012,** *2* (1), 20-35.
10. Ünveren, E. E.; Monkul, B. Ö.; Sarıoğlan, Ş.; Karademir, N.; Alper, E., Solid amine sorbents for CO2 capture by chemical adsorption: A review. *Petroleum* **2017,** *3* (1), 37-50.
11. Rochelle, G. T., Amine scrubbing for CO2 capture. *Science* **2009,** *325* (5948), 1652-1654.
12. Booras, G.; Smelser, S., An engineering and economic evaluation of CO2 removal from fossil-fuel-fired power plants. *Energy* **1991,** *16* (11-12), 1295-1305.
13. Nguyen, T. S.; Dogan, N. A.; Lim, H.; Yavuz, C. T., Amine Chemistry of Porous CO2 Adsorbents. *Accounts of Chemical Research* **2023,** *56* (19), 2642-2652.
14. Kolle, J. M.; Fayaz, M.; Sayari, A., Understanding the effect of water on CO2 adsorption. *Chemical Reviews* **2021,** *121* (13), 7280-7345.
15. Xue, Q.; Liu, Y., Mixed-amine modified SBA-15 as novel adsorbent of CO2 separation for biogas upgrading. *Separation Science and Technology* **2011,** *46* (4), 679-686.

16. Zhao, P.; Zhang, G.; Hao, L., A novel blended amine functionalized porous silica adsorbent for carbon dioxide capture. *Adsorption* **2020,** *26*, 749-764.
17. Fauth, D.; Gray, M.; Pennline, H.; Krutka, H.; Sjostrom, S.; Ault, A., Investigation of porous silica supported mixed-amine sorbents for post-combustion CO2 capture. *Energy & Fuels* **2012,** *26* (4), 2483-2496.
18. Elfving, J.; Kauppinen, J.; Jegoroff, M.; Ruuskanen, V.; Järvinen, L.; Sainio, T., Experimental comparison of regeneration methods for CO2 concentration from air using amine-based adsorbent. *Chemical Engineering Journal* **2021,** *404*, 126337.
19. He, H.; Tang, H.; Chen, X.; Hou, X.; Zhou, X.; Chen, H.; Wu, S.; Wang, S., Structure design of low-temperature regenerative hyperbranched polyamine adsorbent for CO2 capture. *Langmuir* **2018,** *34* (47), 14169-14179.
20. Choi, S.; Gray, M. L.; Jones, C. W., Amine‐tethered solid adsorbents coupling high adsorption capacity and regenerability for CO2 capture from ambient air. *ChemSusChem* **2011,** *4* (5), 628-635.
21. Chullen, C.; Campbell, C.; Papale, W.; Conger, B.; Mcmillin, S. In *Design and Development Comparison of Rapid Cycle Amine 1.0, 2.0, and 3.0*, 46th International Conference on Environmental Systems: 2016.
22. Ouellette, F. A.; Allen, G.; Baker, G. S.; Woods, D. J. *Development and Flight Status Report on the Extended Duration Orbiter Regenerable Carbon Dioxide Removal System*; 0148-7191; SAE Technical Paper: 1993.
23. Filburn, T.; Nalette, T.; Graf, J. *The design and testing of a fully redundant regenerative CO2 removal system (Rcrs) for the shuttle orbiter*; 0148-7191; SAE Technical Paper: 2001.
24. Colling, A. K.; Nalette, T. A.; Cusick, R. J.; Reysa, R. P., Development Status of Regenerable Solid Amine CO 2 Control Systems. **1985**.
25. Filburn, T. P. An investigation into the absorption of carbon dioxide by amine coated polymeric supports. University of Connecticut, 2003.
26. Monje, O.; Nolek, S.; Wheeler, R. In *Ammonia offgassing from SA9T*, 41st International Conference on Environmental Systems, 2011; p 5101.
27. Monje, O.; Brosnan, B.; Flanagan, A.; Wheeler, R. In *Characterizing the adsorptive capacity of SA9T using simulated spacecraft gas streams*, 40th International Conference on Environmental Systems, 2010; p 6063.
28. Smith, F.; Perry, J.; Nalette, T.; Papale, W. In *Development Status of Amine-based, Combined Humidity, CO2, and Trace Contaminant Control System for CEV*, International Conference on Environmental Systems, 2006.
29. Nalette, T.; Reiss, J.; Filburn, T.; Seery, T.; Smith, F.; Perry, J. In *Development of an amine-based system for combined carbon dioxide, humidity, and trace contaminant control*, 35th International Conference on Environmental Systems, 2005.
30. Button, A. B.; Sweterlitsch, J. J. In *Amine swingbed payload testing on ISS*, 44th International Conference on Environmental Systems: 2014.
31. Papale, W.; Nalette, T.; Heldmann, M.; Hidalgo, J. In *An Advanced CO2 Removal System Using Regenerable Solid Amines*, 46th International Conference on Environmental Systems: 2016.
32. Bloom, K.; Conger, B.; Chullen, C. In *Rapid Cycle Amine 4.0 System Development*, 52nd International Conference on Environmental Systems, 2023.
33. Papale, W.; Chullen, C.; Campbell, C.; Conger, B.; McMillin, S.; Jeng, F. In *Continued Development of the Rapid Cycle Amine (RCA) System for Advanced Extravehicular Activity Systems*, International Conference on Environmental Systems, 2014.
34. Todd, K.; Hostetler, J.; Espinosa, N.; Chullen, C. In *Exploration Portable Life Support System Hatch Component Design Challenges and Progress*, 2020 International Conference on Environmental Systems: 2020.
35. Belancik, G.; Chu, L.; Costa, T.; Soundararajan, M. In *Evaluation of Alternative Liquid Sorbents and Additives for Spacecraft CO2 Capture*, 2023 International Conference on Environmental Systems: 2023.
36. Wojtowicz, M. A.; Cosgrove, J. E.; Serio, M. A.; Manthina, V.; Singh, P.; Chullen, C. In *Carbon-Based Regenerable Sorbents for the Combined Carbon Dioxide and Ammonia Removal for the Primary Life Support System (PLSS)*, International Conference on Environmental Systems, 2014.
37. Dutcher, B.; Fan, M.; Russell, A. G., Amine-Based CO2 Capture Technology Development from the Beginning of 2013—A Review. *ACS Applied Materials & Interfaces* **2015,** *7* (4), 2137-2148.
38. Darunte, L. A.; Walton, K. S.; Sholl, D. S.; Jones, C. W., CO2 capture via adsorption in amine-functionalized sorbents. *Current opinion in chemical engineering* **2016,** *12*, 82-90.
39. Meng, F.; Meng, Y.; Ju, T.; Han, S.; Lin, L.; Jiang, J., Research progress of aqueous amine solution for CO2 capture: A review. *Renewable and Sustainable Energy Reviews* **2022,** *168*, 112902.
40. Anderson, W.; Silverstein, R., Structure of Amines by Nuclear Magnetic Resonance Spectrometry. *Analytical Chemistry* **1965,** *37* (11), 1417-1418.
41. Monje, O.; Kenny, P. R.; Sexson, N. A.; Brosnan, B.; Wheeler, R. M. *Subscale Testbed for Characterizing Regenerable Adsorbents used in Air Revitalization of Spacecraft Atmospheres*; 0148-7191; SAE Technical Paper: 2009.
42. Rochelle, G. T., Thermal degradation of amines for CO2 capture. *Current Opinion in Chemical Engineering* **2012,** *1* (2), 183-190.